


ORIGINAL ARTICLE

Quenching-circumvented ergodicity in relaxor

 $\text{Na}_{1/2}\text{Bi}_{1/2}\text{TiO}_3\text{-BaTiO}_3\text{-K}_{0.5}\text{Na}_{0.5}\text{NbO}_3$ Qiumei Wei^{1,2} | Adeel Riaz¹ | Sergey Zhukov¹ | Kathrin Hofmann³ | Mankang Zhu²  |
Yudong Hou²  | Jürgen Rödel¹ | Lalitha Kodumudi Venkataraman¹ ¹Department of Materials and Earth Sciences, Technical University of Darmstadt, Darmstadt, Germany²Key Laboratory of Advanced Functional Materials, Education Ministry of China, College of Materials Science and Engineering, Faculty of Materials and Manufacturing, Beijing University of Technology, Beijing, China³Eduard-Zintl-Institute of Inorganic and Physical Chemistry, Technical University of Darmstadt, Darmstadt, Germany

Correspondence

Lalitha Kodumudi Venkataraman, Department of Materials and Earth Sciences, Technical University of Darmstadt, Darmstadt, Germany. Email: venkataraman@ceramics.tu-darmstadt.de

Funding information

Natural Science Foundation of Beijing Municipality, Grant/Award Number: 2192009 and 2202008; National Natural Science Foundation of China, Grant/Award Number: 52072010 and 51677001; Beijing Talents Project, Grant/Award Number: 2019A25; China Scholarship Council; Deutsche Forschungsgemeinschaft, Grant/Award Number: KO 5948/1-1, SE 941/21-1 and 414311761

Abstract

Quenching alkaline bismuth titanates from sintering temperatures results in increased lattice distortion and consequently higher depolarization temperature. This work investigates the influence of quenching on the ergodicity of relaxor $\text{Na}_{1/2}\text{Bi}_{1/2}\text{TiO}_3\text{-BaTiO}_3\text{-K}_{0.5}\text{Na}_{0.5}\text{NbO}_3$. A distinct departure from ergodicity is evidenced from the increase in remanent polarization and the absence of frequency dispersion in the permittivity response of poled samples. Further, the samples exhibit enhanced negative strain upon application of electric field, indicating proclivity towards correlated polar nanoregions, corroborated by the enhanced tetragonal distortion. As a result, ergodic relaxor $\text{Na}_{1/2}\text{Bi}_{1/2}\text{TiO}_3\text{-6BaTiO}_3\text{-3K}_{0.5}\text{Na}_{0.5}\text{NbO}_3$ exhibits a depolarization temperature of 85°C with a 60% increase in remanent polarization and approximately a threefold increase in remanent strain upon quenching. Quenching-induced changes in the local environment of Na^+ and Bi^{3+} cations hinder the development of ergodicity promoted by the A-site disorder. These results provide new insight into tailoring ergodicity of relaxor ferroelectrics.

KEYWORDS

ferroelectricity/ferroelectric materials, lead-free ceramics, relaxors

1 | INTRODUCTION

The regulation on Restriction of Hazardous substances limits the use of Pb^{2+} in many applications.^{1,2} In response, several material alternatives, namely $(\text{Na}_{1/2}\text{Bi}_{1/2}\text{TiO}_3)$ (NBT)-based,

$\text{K}_{0.5}\text{Na}_{0.5}\text{NbO}_3$ (KNN)-based, BaTiO_3 -based, and BiFeO_3 -based) were identified for specific applications.^{3,4} NBT-based materials are versatile and have been explored for application in solid state ionics,⁵ ultrasonic cleaning,⁶ mechanical energy harvesting,⁷ ultra-high temperature multilayer

This is an open access article under the terms of the Creative Commons Attribution License, which permits use, distribution and reproduction in any medium, provided the original work is properly cited.

© 2021 The Authors. *Journal of the American Ceramic Society* published by Wiley Periodicals LLC on behalf of American Ceramic Society (ACERS).

capacitors⁸ and high strain actuation.^{9–11} Relaxors, such as $(1-x)\text{Na}_{1/2}\text{Bi}_{1/2}\text{TiO}_3-x\text{BaTiO}_3$ (NBT-*x*BT), constitute of polar entities (polar nanoregions, PNRs) below the Burns temperature (T_B) that are dynamic and uncorrelated. Upon cooling, at a critical temperature known as the freezing temperature, $T_f \ll T_B$, the correlation between the PNRs strengthen (remains the same) leading to non-ergodic (ergodic) character, respectively.¹² Ergodicity (non-ergodicity) is defined as the reversible (irreversible) nature of the relaxor to ferroelectric transformation upon application of external stimuli. Relaxor features in NBT-based materials can be modified by chemical substitution or fabricating a multicomponent solid solution^{13–15} and in extreme case, can be transformed to a ferroelectric spontaneously.^{16–18} Recently, quenching has been proposed to promote ferroelectric order in NBT-based materials^{19,20} resulting in an enhanced ferroelectric-relaxor transformation temperature (T_{F-R}). Apart from establishing the practical relevance of the quenching strategy,²¹ leveraging an appropriate starting composition (suitably doped, e.g., one with high a mechanical quality factor, Q) could result in further increase in T_{F-R} , beyond that established by the doping limits, with minimal change in the electromechanical response.¹⁶ The stabilized ferroelectric order in quenched NBT necessarily implies changes in the dynamic nature and correlation length of PNRs. However, such a correlation is incomprehensible from investigating non-ergodic relaxors due to the inherent quasi-static nature of PNRs and their increased correlation length.

The Morphotropic Phase Boundary (MPB) of NBT-*x*BT spans a wide range of compositions^{22,23}; although the core-MPB compositions (6–7 mole% BT) exhibit an average cubic structure,²⁴ with increasing BT content, tetragonal distortions develop in the MPB compositions albeit retaining relaxor features.^{16,17} Assuming a simple composite description of polar (non-cubic) inclusions in a non-polar matrix (cubic), the cubic content decreases with increasing BT content.^{16,25} The average structure is then an additional determining factor in stabilizing a relaxor state. Therefore, two different NBT-*x*BT variants—one with high content of cubic phase at the center of the MPB and another at the edge of the MPB with lower cubic phase content,^{16,25} were chosen for the investigation. NBT-*x*BT-*y*KNN is reportedly known for its giant strain due to the composition-induced cross over from non-ergodic to ergodic relaxor (>2 mole% KNN), characterized by sprout-shaped bipolar strain-field loops in the ergodic state.⁹ The giant strain results due to the presence of a non-polar phase destabilizing the induced ferroelectric order²⁶ and random fields promoting the relaxation of induced ferroelectric order upon application of electric field.²⁷ The aim of this study is to investigate the effect of quenching on both ergodic and non-ergodic NBT-*x*BT-*y*KNN and to establish the influence on the dielectric and piezoelectric properties. Further, the results are rationalized based on the random fields due to the A- and

B-site disorder of NBT-*x*BT-*y*KNN and the increased Bi–O bond length in quenched materials.

2 | EXPERIMENT

$\text{Na}_{1/2}\text{Bi}_{1/2}\text{TiO}_3-x\text{BaTiO}_3-y\text{K}_{0.5}\text{Na}_{0.5}\text{NbO}_3$ (NBT-*x*BT-*y*KNN), where *x* and *y* denote mole% was prepared using the solid state route. Stoichiometric amounts of Na_2CO_3 (99.5%), K_2CO_3 (99%), Bi_2O_3 (99.975%), TiO_2 (99.6%), and Nb_2O_5 (99.9%) (all Alfa Aesar) were milled in ethanol for 12 h using zirconia balls in a planetary ball mill. The dried powders were then calcined at 900°C for 3 h and remilled in ethanol for 6 h. The samples were sintered at 1180°C for 2 h, denoted as FC (short for furnace cooled). Samples were quenched by removing them from the furnace after the sintering dwell time of 2 h and were rapidly cooled in ambient air (denoted as Q, short for quenched). This procedure was determined to decrease the surface temperature to less than 300°C in ~300 s as verified from experiment and simulation.²¹ Two different NBT-*x*BT variants—NBT-6BT and NBT-9BT were chosen. Since the development of ergodicity is dependent on the KNN content, *y* was selected as 3 mole%, since NBT-6BT was demonstrated to exhibit ergodic features beyond 3 mole% KNN.⁹ High resolution diffraction data was acquired from powders (obtained by crushing a pellet and annealing) in transmission geometry using a Stadi P (Stoe & Cie. GmbH) diffractometer equipped with MYTHEN1K (Dectris Ltd.) detector and monochromatized Cu- $K\alpha_1$ radiation ($\lambda = 1.540598 \text{ \AA}$, Ge[111]-monochromator). The microstructure was characterized by scanning electron microscopy (Philips XL30 FEG). The sintered samples were ground and electroded with silver. Prior to all measurements, samples were annealed at 400°C for 30 min to relieve grinding induced mechanical stresses. Poling was done at 6 kV/mm for 20 min. Temperature- and frequency-dependent permittivity measurements were performed using an impedance analyzer (4192A LF; Hewlett-Packard). T_{F-R} was determined from the first anomaly in the temperature-dependent permittivity plots of poled samples. Polarization and strain hysteresis were quantified with a triangular field up to 6 kV/mm at 1 Hz using a Sawyer-Tower circuit equipped with an optical sensor and a temperature stage. The thermally stimulated depolarization current (TSDC) was measured in a short circuit mode, utilizing a constant heating rate of 3 K/min, while the discharge currents were monitored by an electrometer (Model 617; Keithley).

3 | RESULTS AND DISCUSSION

The phase pure perovskite structure of the synthesized materials can be confirmed from Figure 1. Quenching does not

alter the microstructure and the average grain size is 1.2–1.7 μm for both the FC and Q samples (Figure 2).

The ergodicity in NBT-*x*BT-3KNN is exemplified in the temperature- and frequency-dependent dielectric spectra (Figure 3), wherein a strong frequency dispersion is observed for all the samples in the unpoled state at low temperatures.^{28,29} The reversible/irreversible nature of the

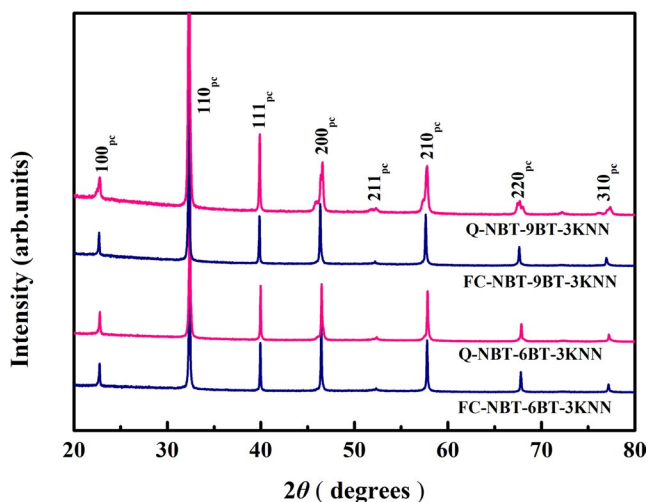


FIGURE 1 X-ray diffraction profiles of furnace-cooled (FC) and quenched (Q) NBT-*x*BT-3KNN [Color figure can be viewed at wileyonlinelibrary.com]

field-induced (poled) relaxor-ferroelectric transformation is established from the permittivity response of poled samples. For FC-NBT-6BT-3KNN, the frequency dispersion is present in both the poled and unpoled state (Figure 3A), indicating ergodic relaxor features. In contrast, FC-NBT-9BT-3KNN exhibits a recognizably weakened frequency dispersion upon poling (Figure 3B). Upon quenching, a stark contrast is observed in the dielectric spectra for both Q-NBT-6BT-3KNN and Q-NBT-9BT-3KNN in the poled state, wherein the frequency dispersion is obviously suppressed at low temperatures, indicative of non-ergodic relaxor character.^{20,30} The first anomaly in the dielectric spectra, characteristic of the ferroelectric-relaxor transformation temperature (T_{F-R}) is 80°C and 136°C for Q-NBT-6BT-3KNN and Q-NBT-9BT-3KNN, respectively (Figure 3C,D). Dielectric loss ($\tan \delta$) in the quenched samples are comparable to FC samples, similar to the observations made previously.²⁰ Note that the maximum in temperature-dependent permittivity, T_m remains majorly unaltered upon quenching and mimics the trend of FC-counterparts (Table 1; Figure 3).

The ergodic nature of FC-NBT-6BT-3KNN is unambiguously established from the pinched and slim polarization-field (P - E) response and sprout-shaped strain-field (S - E) response, with a lower remanent polarization (P_r) and remanent strain (S_r) (Figure 4A,C).³¹ In contrast, Q-NBT-6BT-3KNN is characterized by a 60% increase in P_r and approximately a

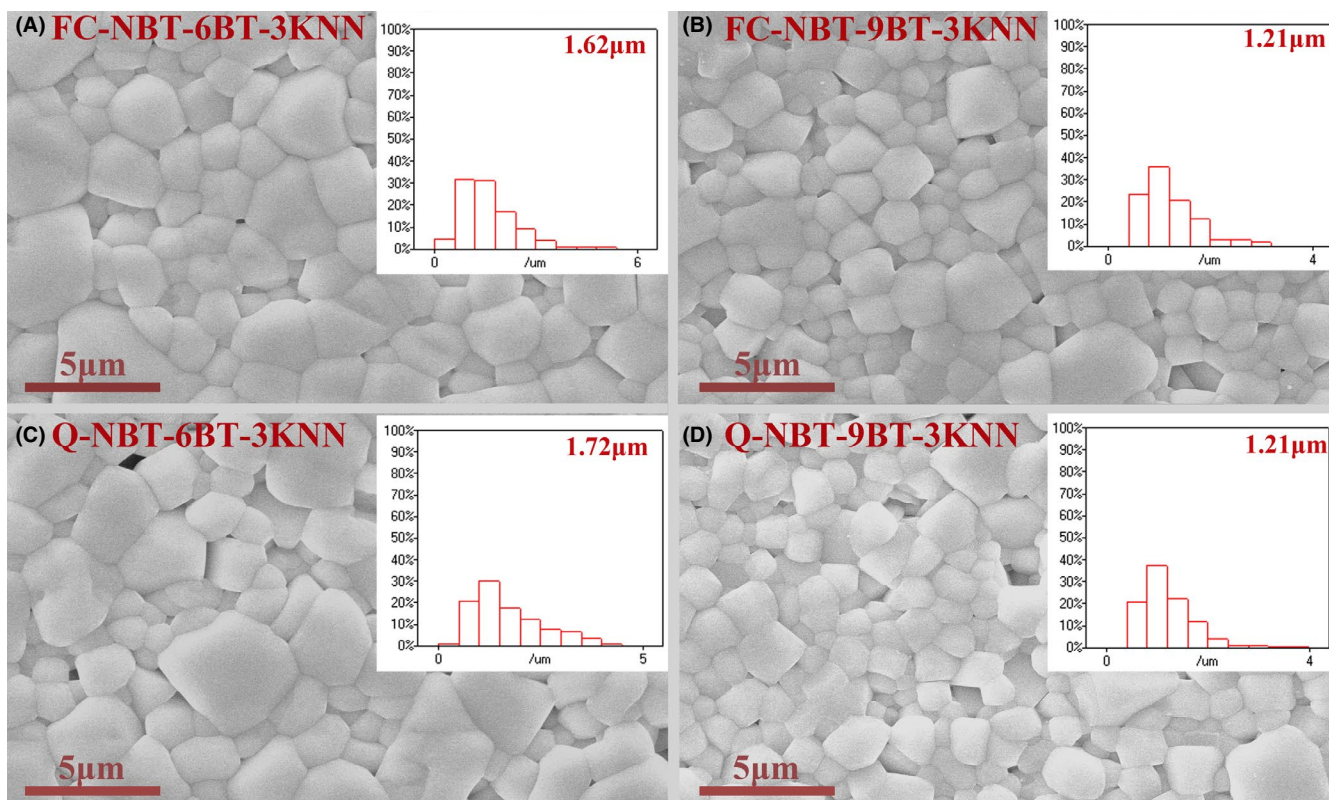


FIGURE 2 Scanning electron microscopy micrographs and the logarithmic normal distribution of grain sizes in the inset for (A, B) furnace-cooled (FC) and (C, D) quenched (Q) samples [Color figure can be viewed at wileyonlinelibrary.com]

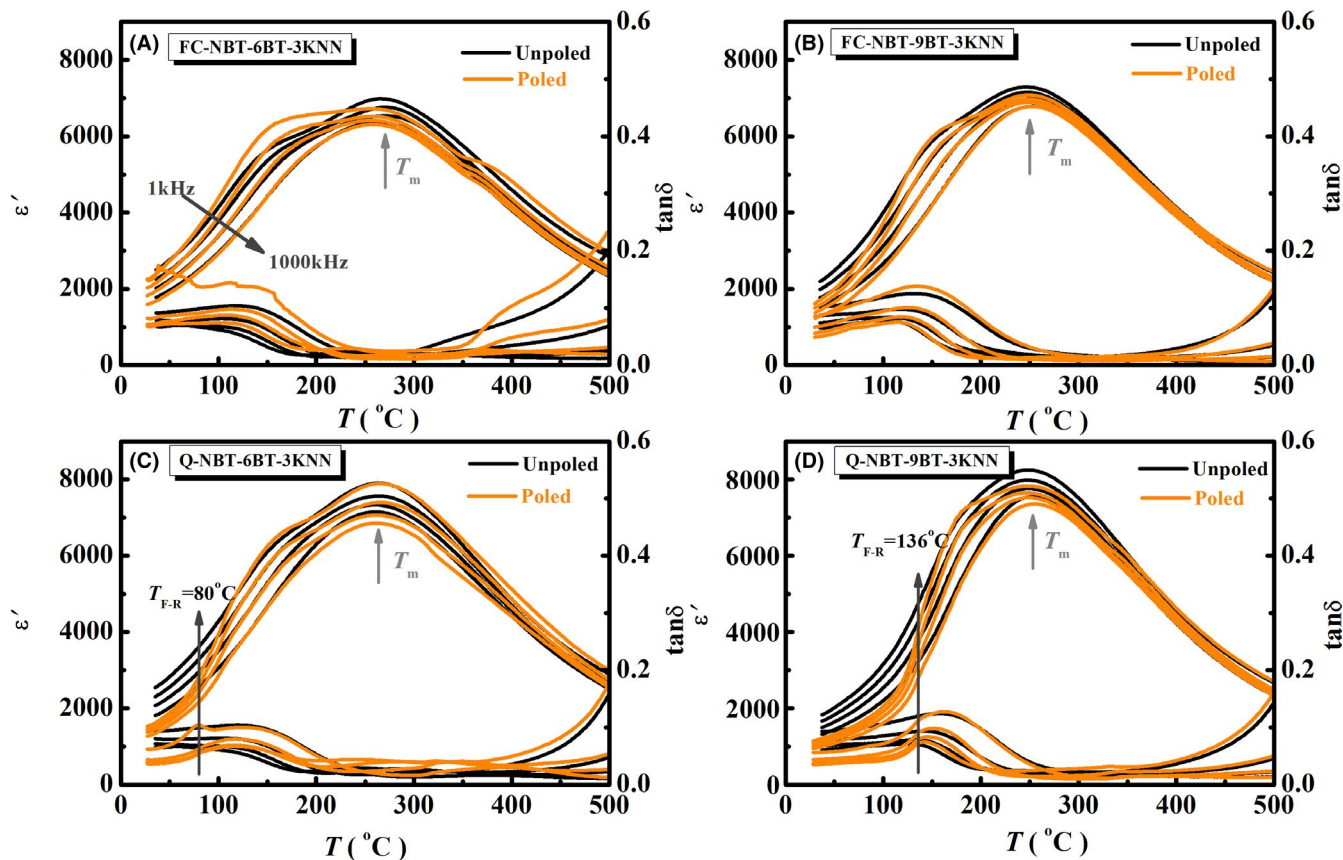


FIGURE 3 Temperature-dependent permittivity and dielectric loss at different frequencies for the (A, B) furnace-cooled (FC) and (C, D) quenched (Q) samples. The poled state was investigated immediately after subjecting the samples to electric field [Color figure can be viewed at wileyonlinelibrary.com]

TABLE 1 Comparison of maximum in permittivity in the temperature-dependent dielectric response (T_m)

Composition	Unpoled/poled T_m (1 kHz), °C	Unpoled/poled T_m (1 MHz), °C	Unpoled/poled ΔT_m (1 kHz–1 MHz), °C
FC-NBT-6BT-3KNN	267/257	261/258	6/1
Q-NBT-6BT-3KNN	263/266	260/261	3/5
FC-NBT-9BT-3KNN	248/250	254/254	6/4
Q-NBT-9BT-3KNN	250/250	254/254	4/4

threefold increase in S_r . In addition, the square-shaped P – E and butterfly shaped S – E response confirm the non-ergodic character of Q-NBT-6BT-3KNN. The increase in P_r signifies increased ferroelectric order for Q-NBT6BT-3KNN. The total strain is not significantly altered, but note that there is a distinctive poling field reflected in the inflection point in the S – E response at 2 kV/mm (Figure 4C). The lower transformation field and sharp inflection for the relaxor→ferroelectric transformation imply the ease of developing long-ranged ferroelectric order upon quenching. FC-NBT9BT-3KNN and Q-NBT9BT-3KNN are non-ergodic relaxors demonstrating similar S – E and P – E response, with comparable P_r and S_r at 30 $\mu\text{C}/\text{cm}^2$ and 0.3%, respectively (Figure 4B,D), in accordance with prior reports.²⁰ Albeit the weak frequency

dispersion in the permittivity response of poled FC-NBT-9BT-3KNN (Figure 4B), the hysteresis response reveals a strong non-ergodic character.

Since quenching the ergodic compositions has been demonstrated to induce non-ergodic features, it becomes imperative to track the thermal depolarization behavior ascertained by the depolarization current and hysteresis response. To this end, TSDC spectra were measured for the samples. FC-NBT-6BT-3KNN exhibits a broad peak in the current density, resulting from the culmination of depolarization of uncorrelated PNRs in the ergodic relaxor (Figure 5A). The resulting polarization obtained from TSDC measurements by integration of depolarization current density over time (Figure 5B) is also weak, in correspondence to the lower P_r as noted

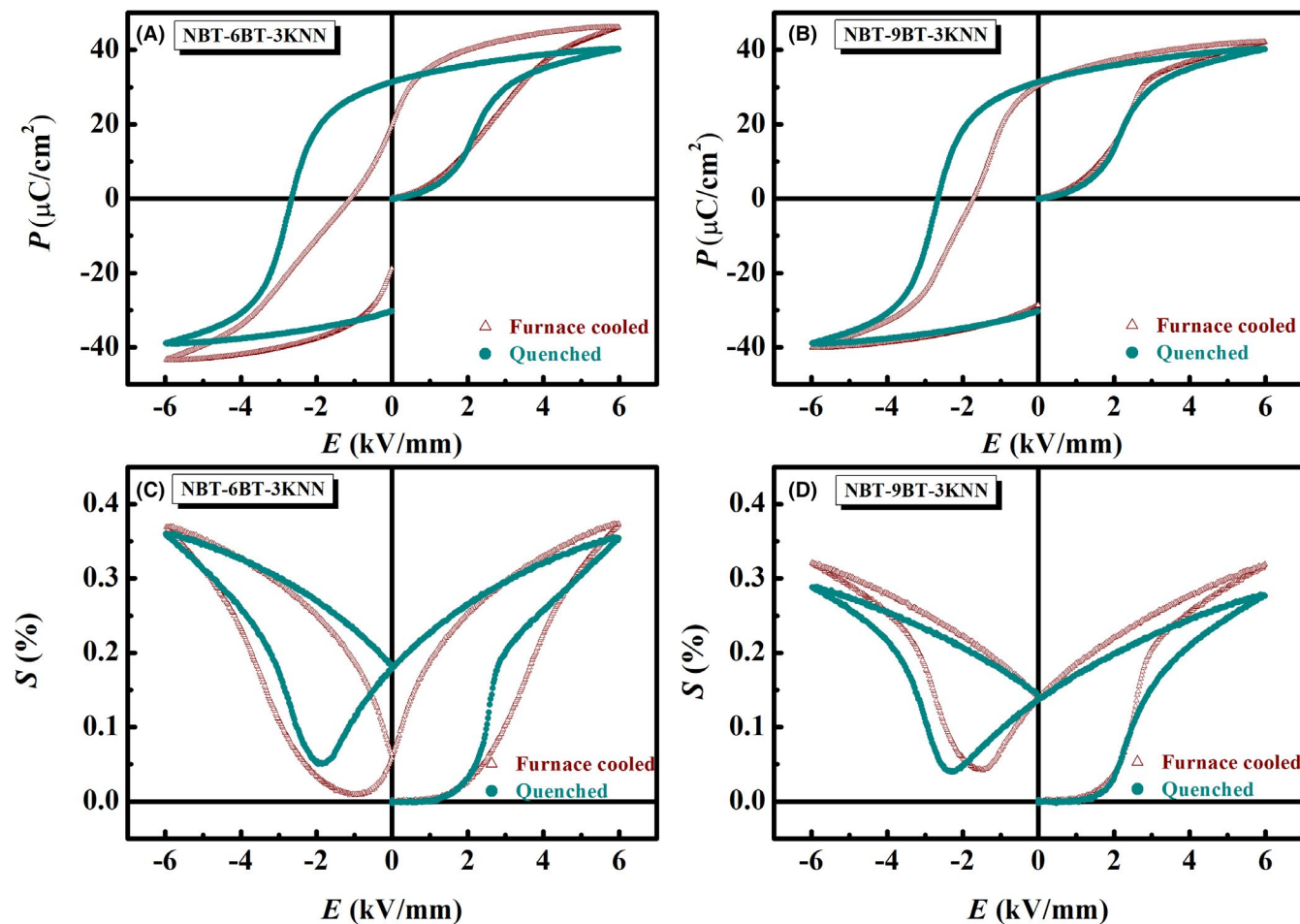


FIGURE 4 (A, B) Polarization and (C, D) strain measured as a function of electric field in the virgin state at 1 Hz for the furnace-cooled and quenched NBT-*x*BT-3KNN [Color figure can be viewed at wileyonlinelibrary.com]

previously. In contrast, all the other samples exhibit a single sharp peak in the depolarization current density, corresponding to the depolarization temperature (T_d). T_d of Q-NBT-6BT-3KNN is 85°C and comparable to T_{F-R} (80°C) established from temperature- and frequency-dependent permittivity response; this is tantamount to the T_d of furnace-cooled non-ergodic NBT-6BT.²⁰ The polarization of NBT-6BT-3KNN exhibits a fourfold increase upon quenching similar to the trend in P_r . Note that, the non-ergodic nature of FC-NBT-9BT-3KNN is evident from the clear depolarization peak at 62°C (Figure 5A). T_d exhibits approximately a twofold increase to 133°C upon quenching NBT-9BT-3KNN. The increase in polarization remains marginal and is in accordance with previous reports on quenching non-ergodic relaxors.²⁰

Figure 6 depicts the high resolution diffraction data obtained from unpoled powders and highlights select diffraction profiles. A singlet in the diffraction profile is expected for cubic symmetry. All the samples indicate non-cubic symmetry reflected in the additional peaks or tails in the diffraction profile (marked by arrows in the figure). However, a notable feature is the development of tetragonal distortions as highlighted in 200_{pc} for Q-NBT-6BT-KNN (Figure 6B).

In the case of NBT-9BT-KNN, although tetragonal distortions are noted for FC, the distortions are more pronounced in the quenched state (Figure 6D). Further, the profile evolution of Q-NBT-6BT-3KNN is comparable to that of FC-NBT-9BT-3KNN, albeit with larger tetragonal distortions for Q-NBT-6BT-3KNN (Figure 6B,D); this reflects as higher T_d for Q-NBT-6BT-3KNN (85°C) in comparison with FC-NBT-9BT-3KNN (62°C) (Figure 5A).

These results establish quenching as a means of tailoring both T_d and ergodicity, as an alternative to chemical modification (higher BT content, doping, new solid solution etc.). Quenching-induced enhancement in tetragonal distortion can be rationalized to result from the anomalous increase in Bi–O bond distance as recently noted in quenched Li-modified-NBT.³²

For NBT-6BT-3KNN, temperature-dependent polarization- and strain-hysteresis response is used to further track the ferroelectric-relaxor transformation (Figure 7). As indicated previously, FC-NBT-6BT-3KNN is in the ergodic state and retains the sprout-shaped S - E loops and slim, pinched P-E loops in the temperature range of investigation (Figure 7A,C).³³ Q-NBT-6BT-3KNN exhibits

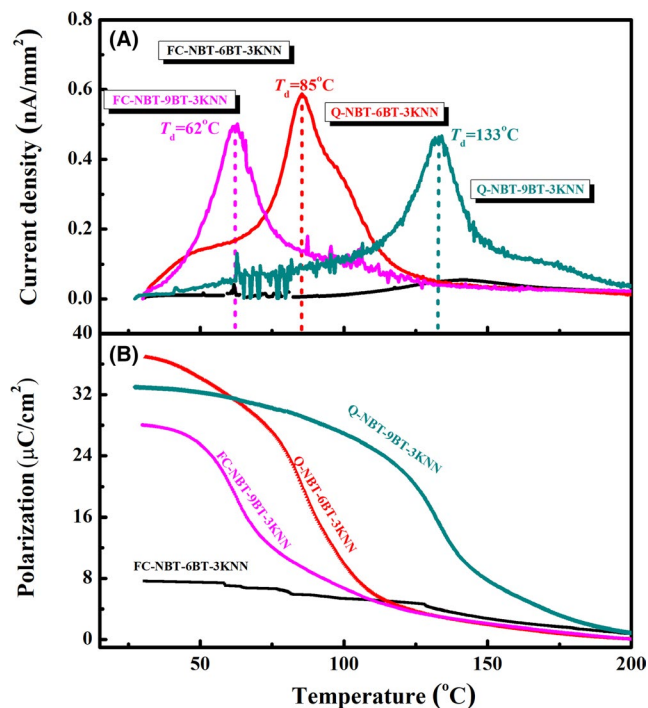


FIGURE 5 (A) Thermally stimulated depolarization current density and (B) calculated polarization from (A) for the furnace-cooled (FC) and quenched (Q) NBT-*x*BT-3KNN [Color figure can be viewed at wileyonlinelibrary.com]

a change of the shape of the hysteresis response close to T_{F-R} (Figure 7B,D). The negative strain (S_{neg}) is close to zero in the ergodic state and is a definite gauge to establish the ferroelectric-relaxor transformation. At room temperature, S_{neg} for FC-NBT-6BT-3KNN is close to zero; however, for Q-NBT-6BT-3KNN, it is roughly three times higher at -0.09% (Figure 8). Further, with increasing temperature, S_{neg} for Q-NBT-6BT-3KNN remains consistently higher than that of FC-NBT-6BT-3KNN and decreases to zero close to T_{F-R} . The temperature at which S_{neg} is zero is marginally higher, since the applied field promotes the ferroelectric order even at T_{F-R} ; however, once the depolarization fields cannot be compensated any longer, the material transforms back to the relaxor state.³⁴

Canonical relaxors upon cooling may result in two extreme possibilities—at the critical freezing temperature, the PNRs get frozen into the non-ergodic state or percolate the material and integrate into a ferroelectric solid.^{28,35} Such transitions into the ferroelectric state has been previously reported for $Pb(Sc_{1/2}Ta_{1/2})O_3$ as a result of cation ordering in the system.³⁶ The stabilization of a ferroelectric order²⁰ upon quenching has been reported previously for non-ergodic NBT-based relaxors, which enhances the T_{F-R} (and T_d) and reflects as an enhanced lattice distortion.^{19,20,32,37,38} Non-ergodic relaxor NBT-9BT-3KNN conforms to this

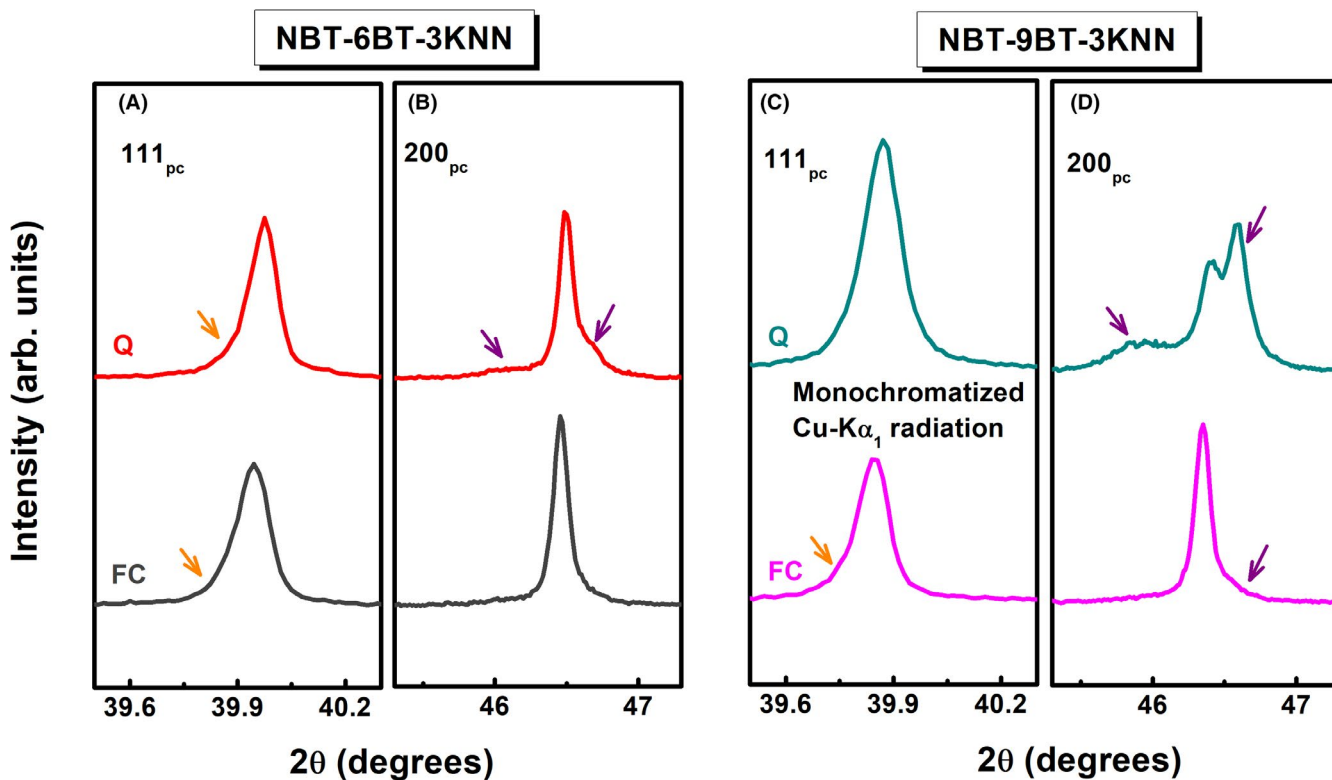


FIGURE 6 Select diffraction profiles of unpoled powder specimen of furnace cooled and quenched (A, B) NBT-6BT-3KNN and (C, D) NBT-9BT-3KNN. The arrows are used to denote deviations resulting from non-cubic distortions. The arrows in 200_{pc} mark the tetragonal distortion [Color figure can be viewed at wileyonlinelibrary.com]

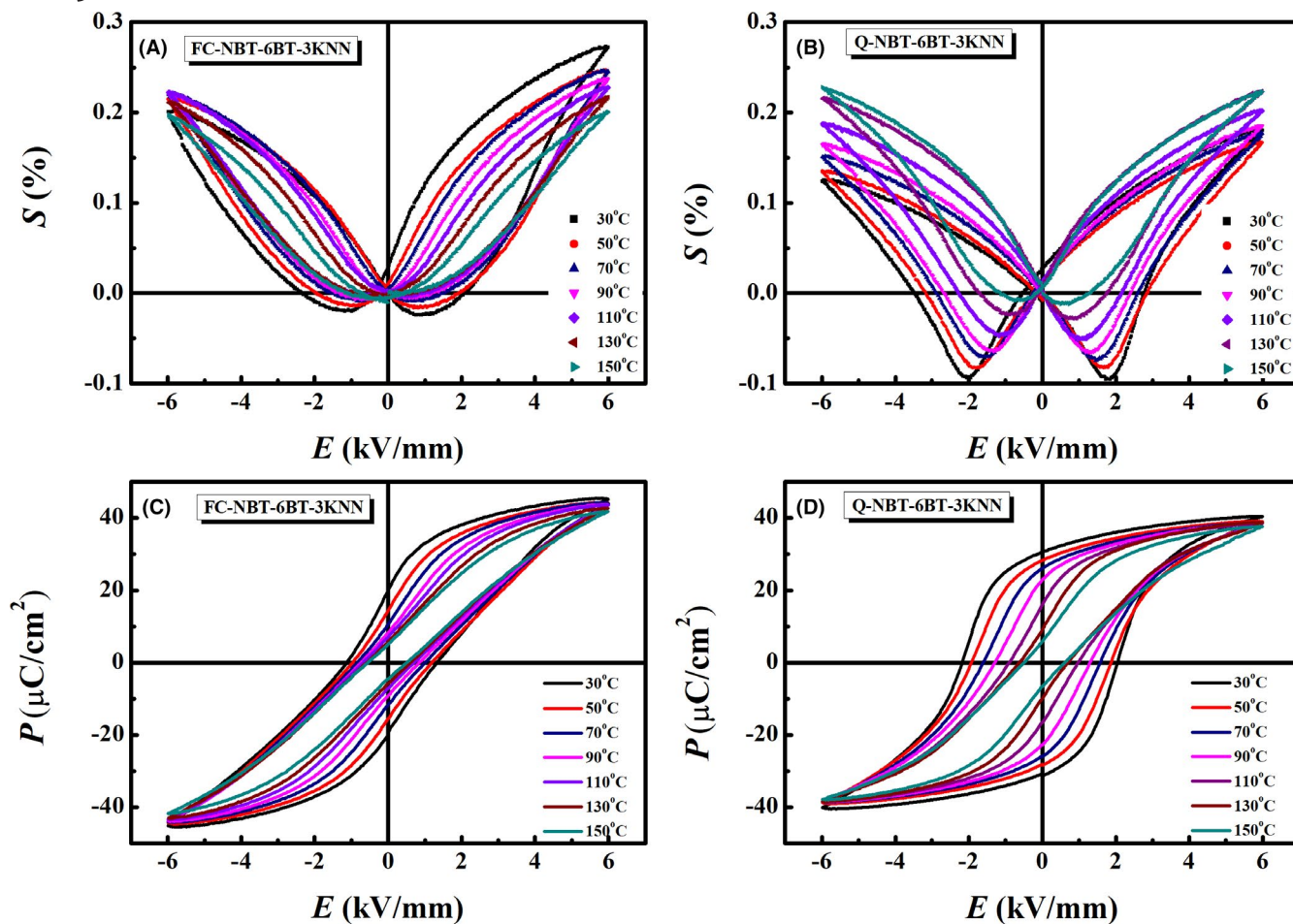


FIGURE 7 Bipolar (A, B) S - E curves and (C, D) P - E loops of furnace cooled (FC) and quenched (Q) NBT-6BT-3KNN measured at different temperatures [Color figure can be viewed at wileyonlinelibrary.com]

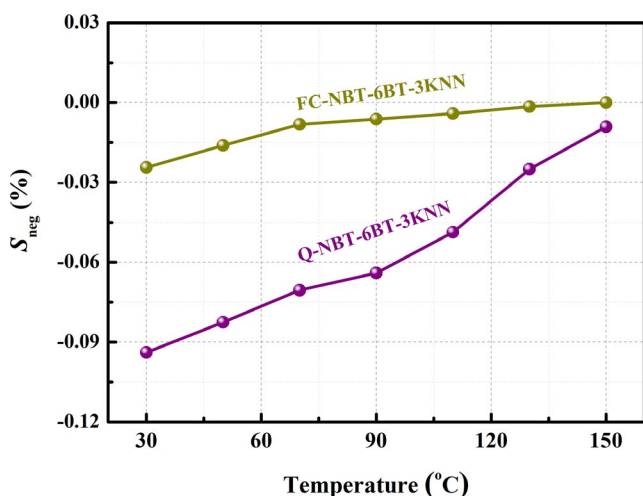


FIGURE 8 Negative strain (S_{neg}) of furnace cooled (FC) and quenched (Q) NBT-6BT-3KNN as a function of temperature [Color figure can be viewed at wileyonlinelibrary.com]

observation, wherein the T_d increased from 62°C to 133°C. The mechanism that enables the ferroelectric equilibrium upon quenching has been debated to result from increased

oxygen vacancy concentration^{20,38} or changes in the local structure²¹ resulting in an enhanced Bi-O off-centered displacements.³² For higher quenching rates, the role of transient thermal stresses has been elucidated based on thermal shock induced microcracking^{39,40} These observations indirectly imply a strong correlation between the PNRs that enable the onset of new polar regions or growth of existing PNRs. This work is an experimental evidence for the same, exemplifying the inception of non-ergodic features upon quenching ergodic samples, reflected in the onset of T_{F-R} and S_{neg} . This then entails an increased correlation between the existing PNRs apart from providing means of tailoring ergodicity as an alternative to new solid solutions or chemical doping. A similar increase in the correlation length of PNRs was facilitated in ergodic relaxor (Ba, Ca)(Ti, Zr)O₃-K_{1/2}Bi_{1/2}TiO₃ by quenching; although driven by chemical heterogeneity (unlike the present study), the quenched samples exhibited enhanced non-cubic (tetragonal) phase fraction as opposed to the slow-cooled specimens.⁴¹

In NBT-6BT, it has been demonstrated that Bi-O and Bi-Ti bond distances feature an abrupt change at T_m but not at T_{F-R} , indicating the transformation from rhombohedral to

tetragonal phase to occur gradually. However, a recent report indicated that quenching results in enhanced Bi^{3+} off-centering as opposed to furnace-cooled specimens,³² which can alter the local structure. In the present work, it was observed that quenching significantly affects $T_{\text{F-R}}$, but does not alter T_{m} (Figure 3; Table 1) and the quenched compositions exhibit an increased tetragonal distortion. This indirectly implies that quenching promotes a stabilization of tetragonal PNRs and increases the ferroelectric order, thus increasing $T_{\text{F-R}}$.

Total scattering X-ray and neutron investigations on the A-site disordered NBT revealed that both Na^+ and Bi^{3+} shift from their average crystallographic position,⁴² with consequently larger Bi–O bond lengths in comparison with Na–O bond distances,⁴³ that can potentially influence the polarizability of the lattice. Quenching non-ergodic relaxor $0.92\text{NBT}-0.08(\text{Bi}_{0.5}\text{Li}_{0.5})\text{TiO}_3$ results in off-centered displacements of Bi^{3+} .³² This work demonstrates that quenching induced long-range order is a potent means to negate the effect of the increased disorder at the A- and B- site random fields due to the introduction of K^+ and Nb^{5+} in $\text{NBT}-x\text{BT}-3\text{KNN}$, that usually promotes ergodicity.

4 | CONCLUSION

Quenching ergodic relaxor $\text{NBT}-6\text{BT}-3\text{KNN}$ is demonstrated to develop non-ergodicity that manifests as onset of $T_{\text{F-R}}$, enhanced negative strain, increased remanent polarization and higher tetragonal distortion. The increase in correlation between the PNRs is rationalized to result from quenching-induced off-centered displacements of Bi^{3+} that circumvents the ergodicity promoted by the A-site disorder.

ACKNOWLEDGEMENTS

Qiumei Wei acknowledges and thanks China Scholarship Council, National Natural Science Foundation of China (grant nos. 52072010, 51677001), Beijing Natural Science Foundation (grant nos. 2192009, 2202008), and Beijing Talents Project (grant no. 2019A25) for financial support. Lalitha K. V. acknowledges and thanks the Deutsche Forschungsgemeinschaft under grant no. KO 5948/1-1 (No.414311761) for financial support. Sergey Zhukov acknowledges and thanks the Deutsche Forschungsgemeinschaft under grant no. SE 941/21-1.

ORCID

Mankang Zhu  <https://orcid.org/0000-0003-0097-908X>

Yudong Hou  <https://orcid.org/0000-0002-0981-3572>

Lalitha Kodumudi Venkataraman  <https://orcid.org/0000-0002-4848-5436>

REFERENCES

- Rödel J, Webber KG, Dittmer R, Jo W, Kimura M, Damjanovic D. Transferring lead-free piezoelectric ceramics into application. *J Eur Ceram Soc.* 2015;35(6):1659–81.
- Bell AJ, Deubzer O. Lead-free piezoelectrics—the environmental and regulatory issues. *MRS Bull.* 2018;43(8):581–7.
- Coondoo I, Panwar N, Kholkin A. Lead-free piezoelectrics: current status and perspectives. *J Adv Dielect.* 2013;03(02):1330002.
- Rojac T, Bencan A, Malic B, et al. BiFeO_3 ceramics: processing, electrical, and electromechanical properties. *J Am Ceram Soc.* 2014;97(7):1993–2011.
- Li M, Pietrowski MJ, De Souza RA, Zhang H, Reaney IM, Cook SN, et al. A family of oxide ion conductors based on the ferroelectric perovskite $\text{Na}_{0.5}\text{Bi}_{0.5}\text{TiO}_3$. *Nat Mater.* 2014;13(1):31–5.
- Tou T, Hamaguti Y, Maida Y, Yamamori H, Takahashi K, Terashima Y. Properties of $(\text{Bi}_{0.5}\text{Na}_{0.5})\text{TiO}_3\text{--BaTiO}_3\text{--}(\text{Bi}_{0.5}\text{Na}_{0.5})(\text{Mn}_{1/3}\text{Nb}_{2/3})\text{O}_3$ lead-free piezoelectric ceramics and its application to ultrasonic cleaner. *Jpn J Appl Phys.* 2009;48(7):07GM03.
- Zhang Y, Liu X, Wang GE, Li Y, Zhang S, Wang D, et al. Enhanced mechanical energy harvesting capability in sodium bismuth titanate based lead-free piezoelectric. *J Alloy Compd.* 2020;825:154020.
- Xu Y, Hou Y, Song B, Cheng H, Zheng M, Zhu M. Superior ultra-high temperature multilayer ceramic capacitors based on polar nanoregion engineered lead-free relaxor. *J Eur Ceram Soc.* 2020;40(13):4487–94.
- Zhang S-T, Kounga AB, Aulbach E, Ehrenberg H, Rödel J. Giant strain in lead-free piezoceramics $\text{Bi}_{0.5}\text{Na}_{0.5}\text{TiO}_3\text{--BaTiO}_3\text{--K}_{0.5}\text{Na}_{0.5}\text{NbO}_3$ system. *Appl Phys Lett.* 2007;91(11):112906.
- Gao X, Dong N, Xia F, Guo Q, Hao H, Liu H, et al. Impact of phase structure on piezoelectric properties of textured lead-free ceramics. *Crystals.* 2020;10(5):367.
- Yoshii K, Hiruma Y, Nagata H, Takenaka T. Electrical properties and depolarization temperature of $(\text{Bi}_{1/2}\text{Na}_{1/2})\text{TiO}_3\text{--}(\text{Bi}_{1/2}\text{K}_{1/2})\text{TiO}_3$ lead-free piezoelectric ceramics. *Jpn J Appl Phys.* 2006;45(5S):4493.
- Viehland D, Chen Y-H. Random-field model for ferroelectric domain dynamics and polarization reversal. *J Appl Phys.* 2000;88(11):6696–707. <https://doi.org/10.1063/1.1325001>.
- Dittmer R, Gobeljic D, Jo W, Shvartsman VV, Lupascu DC, Jones JL, et al. Ergodicity reflected in macroscopic and microscopic field-dependent behavior of BNT-based relaxors. *J Appl Phys.* 2014;115(8):084111.
- Dinh TH, Han H-S, Lee J-S, Ahn C-W, Kim I-W, Bafandeh MR. Ergodicity and nonergodicity in La-doped $\text{Bi}_{1/2}(\text{Na}_{0.82}\text{K}_{0.18})_{1/2}\text{TiO}_3$ relaxors. *J Korean Phys Soc.* 2015;66(7):1077–81.
- Han H-S, Jo W, Rödel J, Hong I-K, Tai W-P, Lee J-S. Coexistence of ergodicity and nonergodicity in LaFeO_3 -modified $\text{Bi}_{1/2}(\text{Na}_{0.78}\text{K}_{0.22})_{1/2}\text{TiO}_3$ relaxors. *J Phys Condens Matter.* 2012;24(36):365901.
- Venkataraman LK, Zhu T, Salazar MP, et al. Thermal depolarization and electromechanical hardening in Zn^{2+} -doped $\text{Na}_{1/2}\text{Bi}_{1/2}\text{TiO}_3\text{--BaTiO}_3$. *J Am Ceram Soc.* <https://doi.org/10.1111/jace.17581>
- Lalitha KV, Hinterstein M, Lee K-Y, et al. Spontaneous ferroelectric order in lead-free relaxor $(\text{Na}_{1/2}\text{Bi}_{1/2})\text{TiO}_3$ -based composites. *Phys Rev B.* 2020;101(17):174108.
- Kumar N, Shi X, Hoffman M. Spontaneous relaxor to ferroelectric transition in lead-free relaxor piezoceramics and the role of point defects. *J Eur Ceram Soc.* 2020;40(6):2323–30.

19. Muramatsu H, Nagata H, Takenaka T. Quenching effects for piezoelectric properties on lead-free $(\text{Bi}_{1/2}\text{Na}_{1/2})\text{TiO}_3$ ceramics. *Jpn J Appl Phys.* 2016;55(10S):10TB07.
20. Lalitha KV, Koruza J, Rödel J. Propensity for spontaneous relaxor-ferroelectric transition in quenched $(\text{Na}_{1/2}\text{Bi}_{1/2})\text{TiO}_3$ - BaTiO_3 compositions. *Appl Phys Lett.* 2018;113(25):252902.
21. Zhang M-H, Breckner P, Frömling T, Rödel J, Lalitha KV. Role of thermal gradients on the depolarization and conductivity in quenched $\text{Na}_{1/2}\text{Bi}_{1/2}\text{TiO}_3$ - BaTiO_3 . *Appl Phys Lett.* 2020;116(26):262902.
22. Ma C, Guo H, Beckman SP, Tan X. Creation and destruction of morphotropic phase boundaries through electrical poling: a case study of lead-free $\text{Bi}_{1/2}\text{Na}_{1/2}\text{TiO}_3$ - BaTiO_3 piezoelectrics. *Phys Rev Lett.* 2012;109(10):107602.
23. Datta K, Roleder K, Thomas PA. Enhanced tetragonality in lead-free piezoelectric $(1-x)\text{BaTiO}_3$ - $x\text{Na}_{1/2}\text{Bi}_{1/2}\text{TiO}_3$ solid solutions where $x=0.05$ - 0.40 . *J Appl Phys.* 2009;106(12):123512.
24. Garg R, Rao BN, Senyshyn A, Krishna PSR, Ranjan R. Lead-free piezoelectric system $(\text{Na}_{0.5}\text{Bi}_{0.5})\text{TiO}_3$ - BaTiO_3 : equilibrium structures and irreversible structural transformations driven by electric field and mechanical impact. *Phys Rev B.* 2013;88(1):014103.
25. Groszewicz PB, Breitzke H, Dittmer R, et al. Nanoscale phase quantification in lead-free $(\text{Bi}_{1/2}\text{Na}_{1/2})\text{TiO}_3$ - BaTiO_3 relaxor ferroelectrics by means of ^{23}Na NMR. *Phys Rev B.* 2014;90(22):220104.
26. Jo W, Granzow T, Aulbach E, Rödel J, Damjanovic D. Origin of the large strain response in $(\text{K}_{0.5}\text{Na}_{0.5})\text{NbO}_3$ -modified $(\text{Bi}_{0.5}\text{Na}_{0.5})\text{TiO}_3$ - BaTiO_3 lead-free piezoceramics. *J Appl Phys.* 2009;105(9):094102.
27. Dittmer R, Jo W, Rödel J, Kalinin S, Balke N. Nanoscale insight into lead-free BNT-BT- x KNN. *Adv Funct Mater.* 2012;22(20):4208-15.
28. Bokov AA, Rayevsky IP. Recent advances in compositionally orderable ferroelectrics. *Ferroelectrics.* 1993;144(1):147-56.
29. Tsurumi T, Soejima K, Kamiya T, Daimon M. Mechanism of diffuse phase transition in relaxor ferroelectrics. *Jpn J Appl Phys.* 1994;33(4R):1959-64.
30. Jo W, Schaab S, Sapper E, et al. On the phase identity and its thermal evolution of lead free $(\text{Bi}_{1/2}\text{Na}_{1/2})\text{TiO}_3$ -6 mol% BaTiO_3 . *J Appl Phys.* 2011;110(7):074106.
31. Jo W, Dittmer R, Acosta M, Zang J, Groh C, Sapper E, et al. Giant electric-field-induced strains in lead-free ceramics for actuator applications—status and perspective. *J Electroceram.* 2012;29(1):71-93.
32. Nagata H, Takagi Y, Yoneda Y, Takenaka T. Correlation between depolarization temperature and lattice distortion in quenched $(\text{Bi}_{1/2}\text{Na}_{1/2})\text{TiO}_3$ -based ceramics. *Appl Phys Express.* 2020;13(6):061002.
33. Zhang S-T, Kouniga AB, Aulbach E, Jo W, Granzow T, Ehrenberg H, et al. Lead-free piezoceramics with giant strain in the system $\text{Bi}_{0.5}\text{Na}_{0.5}\text{TiO}_3$ - BaTiO_3 - $\text{K}_{0.5}\text{Na}_{0.5}\text{NbO}_3$. II. Temperature dependent properties. *J Appl Phys.* 2008;103(3):034108.
34. Sapper E, Novak N, Jo W, Granzow T, Rödel J. Electric-field-temperature phase diagram of the ferroelectric relaxor system $(1-x)\text{Bi}_{1/2}\text{Na}_{1/2}\text{TiO}_3$ - $x\text{BaTiO}_3$ doped with manganese. *J Appl Phys.* 2014;115(19):194104.
35. Tilley RJD. Crystals and crystal structures. John Wiley & Sons; 2006.
36. Chu F, Setter N, Tagantsev AK. The spontaneous relaxor-ferroelectric transition of $\text{Pb}(\text{Sc}_{0.5}\text{Ta}_{0.5})\text{O}_3$. *J Appl Phys.* 1993;74(8):5129-34.
37. Miura T, Nagata H, Takenaka T. Quenching effects on piezoelectric properties and depolarization temperatures of $(\text{Bi}_{0.5}\text{Na}_{0.5})\text{TiO}_3$ -based solid solution systems. *Jpn J Appl Phys.* 2017;56(10S):10PD05.
38. Li Z-T, Liu H, Thong H-C, Xu ZE, Zhang M-H, Yin J, et al. Enhanced temperature stability and defect mechanism of bnt-based lead-free piezoceramics investigated by a quenching process. *Adv Electron Mater.* 2018;1800756.
39. Ren P, Wang J, Wang Y, Lalitha KV, Zhao G. Origin of enhanced depolarization temperature in quenched $\text{Na}_{0.5}\text{Bi}_{0.5}\text{TiO}_3$ - BaTiO_3 ceramics. *J Eur Ceram Soc.* 2020;40(8):2964-9.
40. Takagi Y, Nagata H, Takenaka T. Effects of quenching on bending strength and piezoelectric properties of $(\text{Bi}_{0.5}\text{Na}_{0.5})\text{TiO}_3$ ceramics. *J Asian Ceram Soc.* 2020;8(2):1-7.
41. Al-Aaraji MN, Feteira A, Thompson SP, Murray CA, Hall DA. Effects of quenching on phase transformations and ferroelectric properties of 0.35BCZT-0.65KBT ceramics. *J Eur Ceram Soc.* 2019;39(14):4070-84.
42. Aksel E, Forrester JS, Nino JC, Page K, Shoemaker DP, Jones JL. Local atomic structure deviation from average structure of $\text{Na}_{0.5}\text{Bi}_{0.5}\text{TiO}_3$: combined x-ray and neutron total scattering study. *Phys Rev B.* 2013;87(10):104113.
43. Kitamura N, Hayashi N, Ishida N, Idemoto Y. Local structure in A-site-deficient perovskite $\text{Na}_{0.5}\text{Bi}_{0.5}\text{TiO}_3$ and its effect on electrical conduction. *Chem Lett.* 2019;48(11):1398-401.

How to cite this article: Wei Q, Riaz A, Zhukov S, et al. Quenching-circumvented ergodicity in relaxor $\text{Na}_{1/2}\text{Bi}_{1/2}\text{TiO}_3$ - BaTiO_3 - $\text{K}_{0.5}\text{Na}_{0.5}\text{NbO}_3$. *J Am Ceram Soc.* 2021;104:3316-3324. <https://doi.org/10.1111/jace.17708>